8th US National Combustion Meeting
Organized by the Western States Section of the Combustion Institute
and hosted by the University of Utah
May 19-22, 2013.

Large Eddy Simulation of Complex Thermophysics in Advanced Propulsion and Power Systems

Joseph C. Oefelein

Combustion Research Facility,
Sandia National Laboratories, Livermore, CA 94551-0969

Progress toward application of the Large Eddy Simulation (LES) technique to turbulent multiphase combustion processes typically encountered in advanced propulsion and power systems is presented. The objective is to provide a systematic analysis of current findings and assist in the development of technical performance metrics for model development and validation. Research is currently required to provide both improved multiphase combustion models and improved datasets for validation. Requirements for further model development must be established through detailed analyses of the space-time characteristics of small-scale flame structures and turbulence-chemistry interactions. Concurrently, a refined set of implementation requirements must be established for LES. Steps taken towards these goals are described in the context of a generalized formulation of the filtered conservation equations using an arbitrary filter function that operates on both spatial and temporal scales. Case studies are presented that demonstrate current findings in the treatment of complex thermophysical processes typically present in advanced systems followed by discussion to add perspective on future needs.

1 Introduction

Turbulent flows involving heterogeneous chemically reacting and/or multiphase mixtures (as is the case for all propulsion and power devices) have a variety of complicating factors including highly nonlinear chemical kinetics, small-scale velocity and scalar-mixing, turbulence-chemistry interactions, compressibility effects (volumetric changes induced by changes in pressure), and variable inertia effects (volumetric changes induced by variable composition or heat addition). Coupling between processes occurs over a wide range of time and length scales, many being smaller than can be resolved in a numerically feasible manner. Further complications arise when multiple phases are present due to the introduction of dynamically evolving interface boundaries and the complex exchange processes that occur as a consequence. At the device level, high-performance, dynamic stability, low pollutant emissions, and low soot formation must be achieved simultaneously in highly confined geometries that generate complex flow and acoustic patterns. Flow and combustion processes are highly turbulent (i.e., integral-scale Reynolds numbers of $\mathcal{O}(10^5)$ or greater), and the turbulence dynamics are inherently dominated by geometry or various operating transients. In many cases operating pressures approach or exceed the thermodynamic critical pressure of the fuel (or oxidizer in the case of liquid rocket engines). Operation at elevated pressures significantly increases the system Reynolds number(s) and inherently broadens the range of spatial and temporal turbulence scales over which interactions occur.

No one experimental or numerical technique is capable of providing a complete description of the processes described above. The highest quality experimental diagnostics provide only partial information, and typically at flow Reynolds numbers that are an order of magnitude lower than at the device scale. Modeling and simulation of these processes is always limited by computational power. Even with exascale computing (and beyond), Direct Numerical Simulation (DNS) of the fully coupled equations of fluid motion, transport, and chemical reaction can only be applied over a limited range of turbulence scales (i.e., highly confined domains), in the high wavenumber, low Reynolds number regime of turbulence. Thus, treating the full range of time and length scales at typical device operating conditions must always begin with some form of formal filtering of the governing conservation equations. The Reynolds-Averaged Navier-Stokes (RANS) approximation, for example, employs filtering in time to derive the governing conservation equations for the mean state. For this approach all dynamic degrees of freedom smaller than the largest energy containing eddies are averaged and no information exists to describe interactions between the small-scales. The Large Eddy Simulation (LES) technique, on the other hand, has historically employed spatial filtering to split field variables into time dependent resolved-scale and subgrid- (or subfilter-) scale components. The primary trade-off associated with RANS, LES and DNS is one of accuracy versus computational expense. However, accuracy is not guaranteed as a function of fidelity and it is difficult at times to establish a one-to-one correspondence between canonical approximations and system level processes of interest.

LES provides the formal ability to treat the full range of multidimensional time and length scales in turbulent reacting flows in a computationally feasible manner. The large energetic-scales are resolved directly. The small subgrid-scales are modeled. This allows simulation of the complex multiple-time multiple-length scale coupling between processes in a time-accurate manner. LES is commonly viewed as an engineering tool of the future with the potential to provide useful predictions of combustion at practical conditions and in complex geometries. High-fidelity "first-principles" LES can also serve as a powerful tool for fundamental inquiry into the structure and dynamics of turbulent and/or multiphase combustion processes that are dominated by high-pressure, high Reynolds number, geometrically complex flows. Here, we focus on the latter. The combination of LES, high-performance massively-parallel computing, and advanced experiments offer significant opportunities for synergistic investigations aimed at the development of accurate predictive models. After achieving an appropriate level of validation through direct comparisons between measured and modeled results, information beyond that available from the experiments can be extracted from the LES to gain further insights into both the fundamental physics and the development of advanced engineering models that are both affordable and predictive.

There are several aspects of our LES research that distinguish it from typical approaches. All of the calculations being performed reach beyond the capabilities and resources of many universities and industry and are consistent with a National Laboratory's role of using high-performance computing to enable fundamental exploration of complex combustion phenomena. We apply a single unified theoretical-numerical framework called RAPTOR to all cases being considered. Unlike conventional LES codes, RAPTOR is a DNS solver that has been optimized to meet the strict algorithmic requirements imposed by the LES formalism. The theoretical framework solves the fully-coupled conservation equations of mass, momentum, total-energy, and species for a chemically reacting flow. It is designed to handle high Reynolds number, high-pressure, real-gas and/or liquid conditions over a wide Mach operating range. It also accounts for detailed thermodynamics and

transport processes at the molecular level, and is sophisticated in its ability to handle a generalized model framework in both the Eulerian and Lagrangian frames. A noteworthy aspect of RAPTOR is it was designed specifically for LES using non-dissipative, discretely conservative, staggered, finite-volume differencing. This eliminates numerical contamination of the subgrid models due to artificial dissipation and provides discrete conservation of mass, momentum, energy, and species, which is an imperative requirement for high quality LES. The code has been optimized to provide excellent parallel scalability performance on a variety of computer platforms and is well suited for performing the simulations described here. Details of the baseline theoretical formulation and related subgrid-scale models employed, including a complete description of the governing equations, are given by Oefelein [1] and are thus omitted here for brevity. Representative case studies are given by Oefelein *et al*. [2–12].

2 Results

Results presented here focus on two key areas. The first is coupling between experiments and LES. The second is establishing links between idealized jet flame processes for which significant validation data exists and extension to application relevant processes exhibited at the device scale.

2.1 Coupling between Jet Flow/Flame Experiments and LES

It is widely recognized that accurate representation of scalar gradients is important to a broad range of turbulent flow applications [13–17]. To address this need, a complementary series of experiments to investigate fundamental issues related to thermal gradient structures in turbulent nonpremixed CH_4/H_2/N_2 jet flames has been performed. These flames have been studied extensively [18–22] and used as a benchmark for the TNF Workshop [23]. Results from these investigations have provided significant insights into the small-scale dissipative structure of reacting jets. One-dimensional line Rayleigh thermometry has been used to investigate the effects of spatial resolution and noise on the thermal dissipation spectra [24, 25], and two-dimensional Rayleigh imaging has been used to investigate the detailed structure of the thermal dissipation field [26, 27]. Data was acquired for jet Reynolds numbers of 15,200 (DLR-A) and 22,800 (DLR-B). Using this data, we performed a series of calculations with two primary objectives. The first was to investigate the merits of a new combustion closure. The second was to study scalar mixing.

We continue to investigate the merits of stochastic methods for advanced combustion closures. The objective is to develop first principle models designed specifically for LES, using all the information available from the LES formalism. This is in contrast to conventional RANS-based combustion closures. Recently, a class of reconstruction models has been proposed [28, 29] that combines the purely mathematical approximate deconvolution procedure with physical information from an assumed scalar spectrum to match specific scalar moments. Using this method, a surrogate to the exact scalar field can be estimated such that filtered moments match to a specified order. In principle, the surrogate field can be used to calculate the subgrid contribution of any related nonlinear function. In practice, however, the extent of the nonlinearity limits the accuracy and it has been shown that the method cannot be used reliably to close the filtered chemical source terms directly. It can be used, on the other hand, to obtain highly accurate representations of

Table 1: Grid designed using measured dissipation cutoff wavelengths (Grid A), and two additional by successively coarsening Grid A by a factor of 2 in each coordinate direction (B and C, respectively).

	Downstream of Jet Exit Plane					
Grid	$\mathbf{N}_{axial}$	$\mathbf{N}_{radial}$	$\mathbf{N}_{azimuthal}$	**Total**	**Total Cells**	Δt
A	2592	144	192	71,663,616	82,280,448	0.25 μs
B	1296	72	96	8,957,952	10,285,056	0.50 μs
C	648	36	48	1,119,744	1,285,632	1.00 μs

polynomial nonlinearities such as the subgrid-scale scalar variances. These are precisely the input required to generate correlated subgrid-scale fluctuations stochastically.

Given these findings, we have proposed an extension to the reconstruction approach by coupling it to a stochastic technique. Here, the matrix of subgrid-scale variances obtained via reconstruction are used as input to a Cholesky decomposition to obtain (in the most general case) a correlated approximation of subgrid velocity and scalar fluctuations in time. The modeled instantaneous fields (i.e., $\phi_i = \tilde{\phi}_i + \phi_i''$, where $\tilde{\phi}_i$ represents the resolved-scale contribution of an arbitrary scalar and ϕ_i'' the correlated subgrid-scale fluctuation) are used to evaluate the filtered chemical source terms directly. The filtered source terms are closed by selecting an appropriate chemical kinetics mechanism in the same manner as is done for DNS. The model coefficients are evaluated locally in a manner consistent with the dynamic modeling procedure. The only adjustable parameters are the grid resolution, integration time-step, and boundary conditions. In the limit as the grid resolution and time-step approach the smallest relevant scales, subgrid contributions approach zero and the solution converges to a DNS. A novel feature of the "Stochastic Reconstruction Model" is that it naturally accounts for multiple-scalar mixing and incorporates the fundamental progress variables associated with a given chemical kinetics mechanism directly.

To establish the baseline accuracy of the Stochastic Reconstruction Model, we performed an LES of the DLR-A flame using the 12-step, 16-species reduced chemical mechanism for methane-air developed by J.-Y. Chen (U.C. Berkeley). The overall domain is 110 by 40 jet diameters ($88\ cm\ \times\ 32\ cm$) and includes the burner geometry. The inner diameter of the burner nozzle is $8.0\ mm$. The outer nozzle surface is tapered to a sharp edge at the exit. The burner nozzle itself is 10 diameters long. Cells upstream of the nozzle exit are clustered inside the burner to accurately treat the turbulent time-dependent boundary layer, and outside of the burner to accurately treat the coflow of air that surrounds it. A novel feature of our approach was to design the LES grids using the measured dissipation spectrum cutoff length scales provided by Frank *et al*. [27]. For the baseline case considered here, we used Grid B listed in Table 1. This distribution provides the level of fidelity required to perform a "wall-resolved" LES, where the boundary layer dynamics are resolved. The first cell from the wall is within a y^+ value of 1, the first 16 cells are within the interval $0 < y^+ < 30$, and the transverse grid spacing is set so Δx^+ and Δz^+ are both less than 50.

The bulk jet and coflow velocities for the DLR-A case are 42.2 and $0.3\ m/s$, respectively. The burner section is long enough to assume that a fully-developed turbulent profile exists inside the jet nozzle. With the added assumption that all wall surfaces are hydraulically smooth, we use the LES solver itself to drive a fully-developed turbulent boundary layer inside the duct. Time-evolving velocity profiles are generated by recycling the fields from radial planes at an axial distance of 2

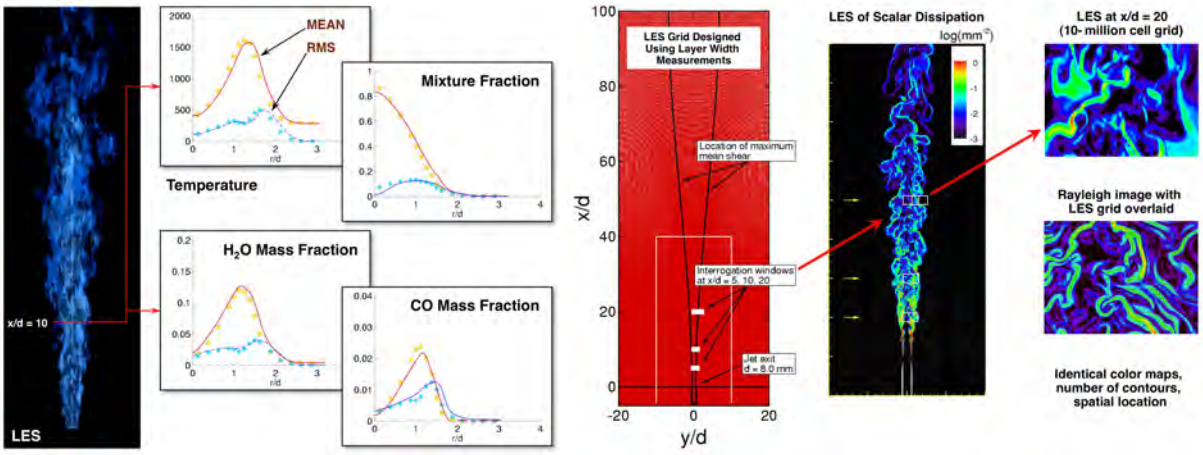

Figure 1: Left is a LES of the DLR-A flame with representative comparisons between experimentally measured (symbols) and modeled (lines) results. Right is a cross-section of Grid B (see Table 1) showing key topological features, the location of 2D imaging windows, the instantaneous structure of the dissipation field from LES, and close-ups of the structure from LES at $x/d = 20$ compared to an experimental image.

dimensionless units upstream of the jet exit. The stripped fields are then imposed at the burner inlet 10 units upstream along with a non-reflecting pressure condition. Far-field, force-free conditions are imposed elsewhere. Figure 1 (left) shows a representative instantaneous solution with comparisons between measured Raman/Rayleigh/CO-LIF line images (symbols) and modeled (lines) mean and RMS profiles. In all cases, the agreement is within 10%.

In addition to the comparisons above, we have also used the DLR-A configuration to work toward a systematic approach for coupling laser-based imaging measurements and LES. Coupling of imaging measurements and LES provides a unique opportunity for understanding the dynamics of turbulence-flame interactions and the related structural dynamics of mixing. For example, imaging of the thermal and scalar dissipation fields acquired by Frank *et al.* [26, 27] reveal the convoluted inhomogeneous structure of the fine-scale scalar mixing processes. The orientation and morphology of the structures are anisotropic and vary significantly from the low-temperature regions near the jet centerline to the high temperature reaction zone. Using these data, we have performed a systematic analysis of the instantaneous structures using the set of grids summarized in Table 1. Details of the study are given by Frank, Kaiser and Oefelein [30]. Representative results are provided in Fig. 1 (right), which shows a cross-section of Grid B and location of the imaging windows, the corresponding instantaneous structure of the dissipation field from LES, and close-ups of the dissipation structures from LES at $x/d = 20$ compared to a corresponding experimental image.

Analysis of the data illustrate how the actual fields of interest (e.g., mixture fraction, scalar dissipation) and the associated physical scales relate to key numerical parameters such as grid spacing, filter size, time-step, and resultant structural dynamics exhibited by LES. For example, on the coarsest grid in the example above (Grid C), there is no correlation at all between the structural characteristics of the measured and computed instantaneous fields even though accurate time-averaged fields are produced. As the spatial and temporal resolution is consistently increased, however, we begin to see an increasing correspondence to the actual structural characteristics of the fields. Applying the resolution associated with Grid A in the example above provides a near one-to-one

correspondence between the measured and simulated results in the distribution of filament diameters observed in respective interrogation windows when sampled over time. This highlights the two operational extremes that LES can be bracketed by. At coarser resolution levels, as is typically the case for engineering calculations to reduce cost, instantaneous fields are only represented by resolved-scale pseudo-structures that emulate the bulk effect of a localized ensemble of structures in the actual field. At high resolution levels, the simulated instantaneous fields begin to provide a more structurally correct representation of the fields. Naturally, fidelity in representing various processes degrades as the statistical moments (e.g., mean, variance, skewness) of the quantities of interest increase. Understanding the relationship between the actual small-scale dynamics and how they are represented by LES (resolution, critical numerical and physical scales, statistical averages) is currently an active and ongoing area of our research.

2.2 Extension to Application Relevant Processes Exhibited at the Device Scale

The importance of understanding and predicting multiphase flow phenomena such as liquid injection, atomization, and spray dynamics in advanced propulsion and power systems is widely recognized. Liquid injection processes largely determine fuel-air mixture formation, which governs the detailed evolution of chemical kinetic processes and ultimately combustion. The lack of accurate models is a major barrier toward the design of optimized, clean, high-efficiency, low-emissions combustion systems. In this section, we focus on pertinent research issues related to both sprays and high-pressure supercritical flows. In particular, there are two extremes in pressure that must be considered in modern devices. At low subcritical operating pressures, the classical situation exists where a well-defined molecular interface separates the injected liquid from ambient gases due to the presence of surface tension. Interactions between dynamic shear forces and surface tension promote primary atomization and secondary breakup processes that evolve from a dense state, where the liquid exists as sheets, filaments, or lattices intermixed with sparse pockets of gas; to a dilute state, where drop-drop interactions are negligible and dilute spray theory can be used. When operating pressures exceed the critical pressure of the injected liquid, however, the situation can become quite different. Under these conditions, interfacial diffusion layers can develop as a consequence of both vanishing surface tension forces and broadening gas-liquid interfaces. These interfaces eventually enter the continuum length scale regime and disappear as interfacial fluid temperatures rise above the critical temperature of the local mixture. Lack of inter-molecular forces, coupled with broadening interfaces, promote diffusion dominated mixing processes prior to atomization. As a consequence, injected jets evolve in the presence of exceedingly large but continuous thermo-physical gradients in a manner markedly different from classical assumptions. The key phenomenological focal points that need to be considered are summarized in Table 2. Below we show two examples aimed at addressing a subset of these phenomena with LES.

2.2.1 Systematic Treatment of Dilute Spray Dynamics

Obtaining high-fidelity solutions of reacting sprays hinges on the application of methods and models that accurately describe momentum coupling and subgrid-scale modulation of turbulence, mass and energy coupling and subgrid-scale scalar mixing, and the turbulent combustion processes in-

Table 2: Key phenomenological focal points for advanced treatment of reacting multiphase flows.

1. Primary atomization (sheet, filament and lattice formation)
2. Secondary breakup (particle deformation and coalescence processes)
3. Dilute spray dynamics
a. Drop dispersion
b. Multicomponent drop vaporization
c. Two-way coupling between the gas and dispersed liquid phase
– Turbulence modulation (damping of turbulence due to particle drag effects)
– Turbulence generation (production of turbulence due to particle wakes)
4. High-pressure supercritical phenomena
a. Real-fluid equations of state, detailed thermodynamics and transport
b. Multicomponent mixtures, extreme property gradients, preferential transport
5. Turbulent mixed-mode combustion
a. Thermodynamic non-idealities, transport anomalies
b. Complex hydrocarbon chemistry, high-pressure chemical kinetics

duced as a consequence. As part of an effort to treat these phenomena systematically, we have performed a series of LES studies that focus on a swirling particle-laden flow in a model coaxial combustion chamber. Calculations have been performed and compared to the experimental data acquired by Sommerfeld *et al*. [31–33]. Sommerfeld *et al*. provides detailed measurements of swirling particle-laden flow in a model combustion chamber that consists of a sudden pipe expansion with a centered and annular jet discharging into a cylindrical test section. The experimental measurements were acquired using a one-component phase-Doppler-anemometer (PDA) to obtain mean and RMS gas-phase and particle-phase statistics of velocity and particle size. These data provide excellent benchmark cases for validation of LES in a turbulent swirling-flow environment with well-defined boundary conditions. They provide a way to systematically validate LES models for unsteady dilute spray dynamics without having to simultaneously treat more complex issues related to primary atomization and secondary breakup.

Figures 2 and 3 show representative LES results calculated using RAPTOR. Comparisons with the available data have demonstrated the baseline accuracy of the current framework for treating turbulent dispersion of dilute sprays in a complex recirculating swirling flow that has characteristics relevant to gas turbine (and similar) combustors. We have established a groundwork for simulating complex wall bounded turbulent flows, non-reacting particle-laden flow, and recirculating swirling flow and highlighted a systematic approach for validating the accuracy of LES in a progressive manner with well-defined and carefully implemented boundary conditions. The validated case study provides a mechanism to establish baseline numerical capabilities, to gain a clearer understanding of the effectiveness and feasibility of current models, and to gain a more quantitative understanding of relevant modeling issues by analyzing the characteristic parameters and scales of importance. Details can be found in the paper by Oefelein *et al*. [5]. Future work will focus on continued systematic assessments and validation of the physical models for sprays. In particular, we will focus on particle-turbulence interactions, with emphasis placed on the effects of

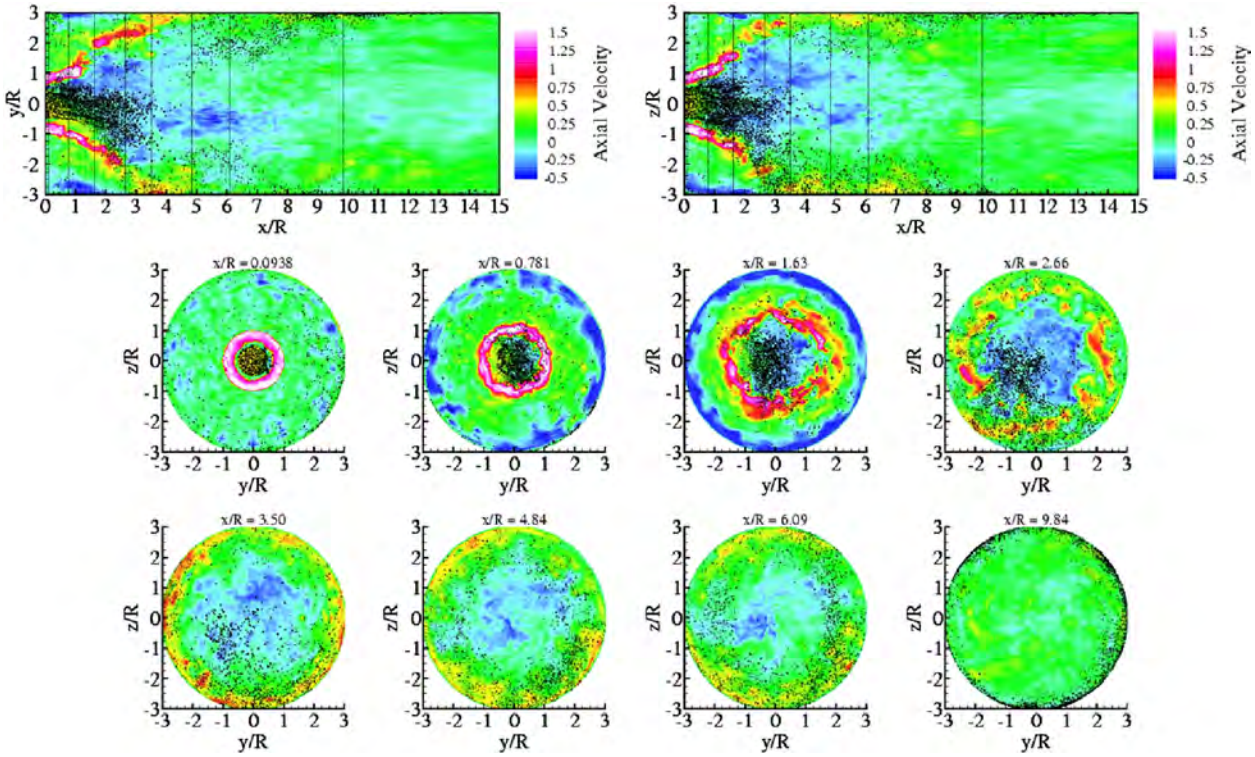

Figure 2: Instantaneous particle distribution superimposed on the corresponding turbulent velocity field (Case 2). The calculations were performed using RAPTOR, see Oefelein *et al.* [5] for details.

gas-phase velocity fluctuations on particle dispersion characteristics, the preferential concentration of particles, and the influence of particles on the turbulence energy spectra [34–37].

2.2.2 Detailed Treatment of High-Pressure Supercritical Phenomena

Research over the past decade has provided significant insights into the structure and dynamics of multiphase flows at high pressures [4, 38–48]. Most of this research has been done in the context of liquid-rocket propulsion, which involves direct injection of both liquid fuel and oxidizer into the combustion chamber. However, the observed trends are equally valid for other liquid fueled devices. Over the past several years, we have focused on treatments of multiphase flows at high pressures with emphasis on complex hydrocarbon fuels. We considered a series of direct injection processes at conditions relevant to Diesel engines, where the fuel is injected at conditions that exceed its thermodynamic critical pressure. A key aspect of this work is the development of both the theory and numerical methods required to handle real-fluid thermodynamics and transport of the fuels and resultant multicomponent mixtures.

The real-fluid property evaluation scheme employed in RAPTOR is designed to account for thermodynamic non-idealities and transport anomalies over a wide range of pressures and temperatures. The scheme is comprehensive and intricate, thus only a skeletal description is given here. The extended corresponding states model [49, 50] is employed using either Benedict-Webb-Rubin (BWR) or cubic equations of state to evaluate the pressure-volume-temperature (PVT) behavior

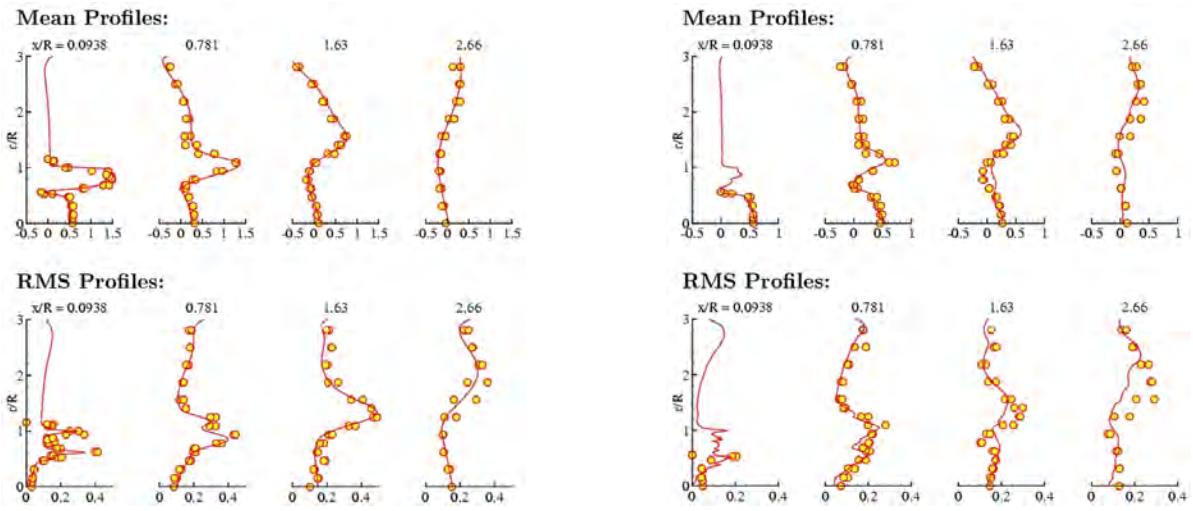

Figure 3: Time-averaged profiles of the dimensionless gas-phase (a) and particle-phase (b) velocity fields. Case 2, symbols represent measured data from Sommerfeld *et al.*[31–33], lines represent LES results.

of the inherent dense multicomponent mixtures. Use of modified BWR equations of state in conjunction with the extended corresponding states principle has been shown to provide consistently accurate results over the widest range of pressures, temperatures, and mixture states, especially at near-critical conditions. A major disadvantage of the BWR equations, however, is that they are not computationally efficient. Cubic equations of state can be less accurate, especially for mixtures at near-critical or saturated conditions, but are computationally efficient. Experience has shown that both the Soave-Redlich-Kwong (SRK) and Peng-Robinson (PR) equations, when used in conjunction with the corresponding states principle, can give accurate results over the range of pressures, temperatures and mixture states typically of interest. SRK coefficients are fit to vapor pressure data and thus more suitable for conditions when reduced temperatures are less than one. PR coefficients, on the other hand, are more suitable for conditions when reduced temperatures are greater than one. A summary of the cubic equations of state is given by Reid *et al.* [51, Chapter 3].

Having established an analytical representation for real mixture PVT behavior, thermodynamic properties are obtained in two steps. First, respective component properties are combined at a fixed temperature using the extended corresponding states methodology outlined above to obtain the mixture state at a given reference pressure. A pressure correction is then applied using departure functions of the form given by Reid *et al.* [51, Chapter 5]. These functions are exact relations derived using Maxwell's relations (see for example VanWylen and Sonntag [52, Chapter 10]) and make full use of the real mixture PVT path dependencies dictated by the selected equation of state. Standard state properties are obtained using the databases developed by Gordon and McBride [53] and Kee *et al.* [54]. Likewise, viscosity and thermal conductivity are obtained using the extended corresponding states methodologies developed by Ely and Hanley [55, 56]. Mass and thermal diffusion coefficients are obtained using the methodologies outlined by Bird *et al.* [57] and Hirschfelder *et al.* [58] with the corresponding states methodology of Takahashi [59].

To facilitate the analysis presented below, the real-fluid framework described above is combined with Vapor-Liquid Equilibrium (VLE) and Linear Gradient (LG) theory to calculate the detailed

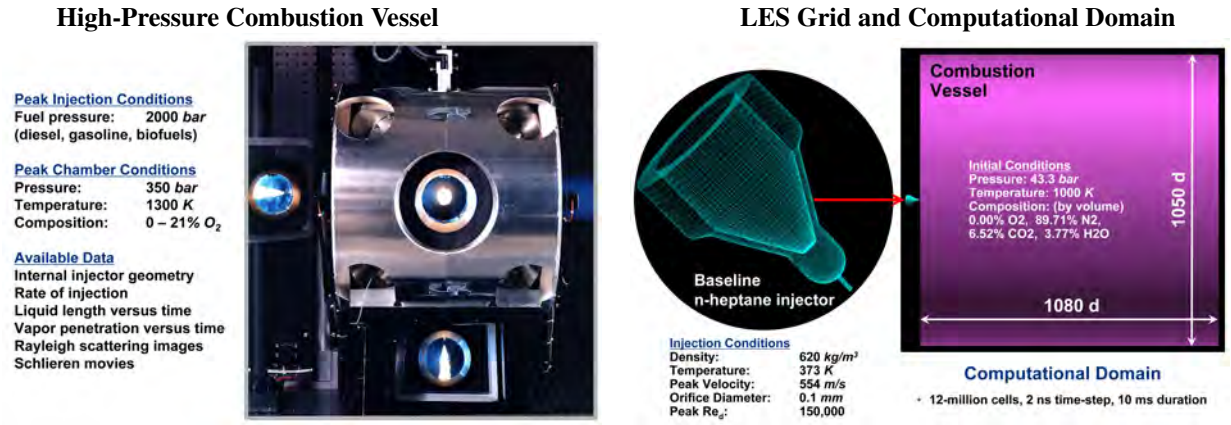

Figure 4: Photograph of the Sandia high-pressure combustion vessel (left) and computational domain used for LES (right). The injector is mounted at the head-end of the vessel, as indicated by the red arrow.

vapor-liquid interfacial structure for the multicomponent mixtures of interest. LG theory provides a thermo-mechanical model of continuous fluid media. At equilibrium, the model has been shown to be equivalent to mean-field molecular theories of capillarity. The foundations of this theory were established by van der Waals in 1894 and reformulated later by Cahn and Hilliard [60]. Gradient theory has been successfully applied to a wide variety of fluids including vapor-liquid and liquid-liquid interfaces associated with hydrocarbon mixtures, polar compounds, and polymers. Recently, the LG model has been successfully compared to Monte Carlo molecular simulations of vapor-liquid and liquid-liquid interfaces aimed at capturing both surface tension and the details of the corresponding molecular interfacial structures [61–63]. Using LG theory, both surface tension and the interface thickness can be calculated through integration along the interfacial density profile.

Using a combination of LES, the real-fluid model, VLE, and LG theory, we have performed a series of studies aimed at understanding the effects of pressure on interfacial injection dynamics. To facilitate the analysis, we considered the operating conditions associated with two key experiments being studied by Pickett *et al*. [64]; namely the "Spray-H (n-heptane)" and "Spray-A (n-dodecane)" cases. These experiments are designed to emulate conditions typically observed in a Diesel engine. Calculations were performed by identically matching the experimental operating conditions, injector geometry, and combustion chamber. The experimental apparatus, corresponding computational domain, and key operating conditions for the Spray-H case are shown in Fig. 4. The experiment involves a liquid n-heptane jet injected into a hot quiescent mixture of gaseous products. For the case considered here, all the oxygen has been consumed to prevent the onset of combustion so we can focus on thermo-physical processes associated with injection. The ambient gas composition in the vessel is conditioned to provide an inert composition of N_2, CO_2, and H_2O. The actual mole fractions of these components are summarized in Fig. 4.

The thermodynamic characteristics of n-heptane are shown in Fig. 5. Its critical point is $540\ K$, $27.4\ bar$. Thus, n-heptane is injected into the chamber as a compressed liquid (i.e., supercritical with respect to pressure, subcritical with respect to temperature). The transient jet pulse is modeled to closely approximate the actual experimental conditions. This produces a peak bulk velocity of $554\ m/s$ and corresponding jet Reynolds number of $150,000$ inside the injector nozzle. The quasi-steady portion of the pulse lasts for $6.66\ ms$. At $6.69\ ms$ the jet ramps down to zero velocity, with

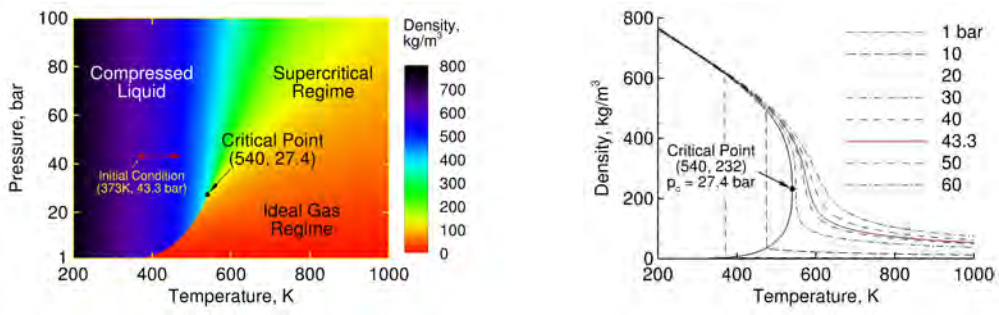

Figure 5: Thermodynamic characteristics of n-heptane showing key regimes and its initial state when injected. N-heptane enters as a compressed liquid and is heated at supercritical pressure.

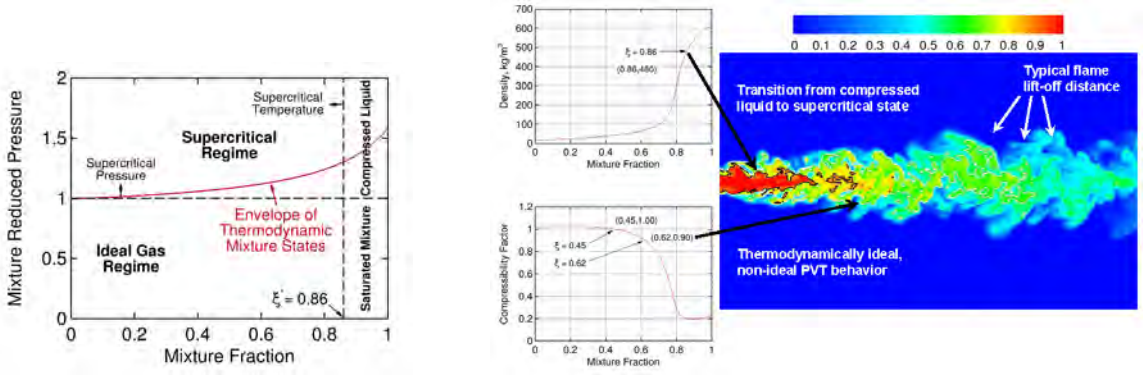

Figure 6: Envelope of mixture states predicted as a function of mixture fraction ξ (left) and contour plot showing a representative LES prediction of mixture fraction (right). Iso-lines mark the transition of the mixture from a compressed liquid to supercritical state (black) and separation between regions of non-ideal and ideal fluid behavior (white).

the end of injection occurring at $6.93\ ms$. Representative results are shown in Fig. 6. On the left we show a plot of the entire envelope of mixture states on a thermodynamic regime diagram. Trends demonstrate that the mixing path associated with all states throughout the duration of injection never crosses the liquid-vapor regime (i.e., the mixture is never saturated). Instead, n-heptane is injected as a compressed liquid and the interfacial mixing layer dynamics are locally supercritical. Surface tension effects are typically assumed to be negligible under such conditions, which implies that classical first order vapor-liquid phase transitions (as are typically assumed) do not occur. Instead, processes dominated by surface tension such as primary atomization, secondary breakup, and the presence of distinct drops are negligible.

The contour plot shown on the right in Fig. 6 provides details of the time evolving mixture. Here, a typical instantaneous mixture fraction field is shown with iso-lines that mark the thermodynamic transition of the mixture from a compressed liquid to a supercritical state (black), and the separation between non-ideal and ideal fluid behavior (white). Results demonstrate for the first time that the injected n-heptane enters the combustion chamber as a compressed liquid, not as a spray, and is heated at supercritical pressure. This implies 1) that applying the ideal gas assumption just prior to autoignition in these types of flows is not valid, and 2) the classical view of spray atomization and secondary breakup processes as an appropriate model (as is widely assumed currently) is

questionable for this case. Instead, non-ideal real-fluid behavior associated with the dense liquid jet must be taken into account. Details related are given by Oefelein *et al.* [10–12, 65].

Results shown here provide the framework necessary for detailed analysis of real-fluid thermodynamics and transport at high-pressures. In particular, subgrid-scale variances associated with the equation of state itself (which are typically ignored), must be considered as part of accurate closures for scalar mixing in LES. Additionally, non-ideal thermodynamics and transport associated with local mixtures will have a profound effect on chemical kinetics and must also be considered along with development of high-pressure chemical mechanisms for complex hydrocarbon fuels.

3 Discussion

The results shown above are intended to illustrate various aspects of progress toward application of LES to turbulent multiphase combustion processes typically present in advanced propulsion and power systems. The representative case studies demonstrate current findings in the treatment of the complex thermophysical processes and provide examples of future needs. To facilitate advance model development, however, application of LES must be augmented with the development of quality assessment techniques and related implementation requirements to effectively minimize and/or control the many potential sources of error.

Development of LES is complicated by the interdependence of different subgrid models, competition between modeling and numerical errors, model variability, and numerical implementation. Errors and ambiguities are multiplying, and control of accuracy has become a critical aspect in the development of predictive LES. When accuracy is not sufficient, results can be misleading and intractably erroneous due to factors such as poor numerics, poor grid quality, lack of appropriate spatial or temporal resolution, ill-posed boundary conditions, and inaccurate models. Given the myriad of competing interdependencies that affect solution accuracy, time to solution, and the overall confidence in the predictive quality of LES, a current goal is to establish robust performance metrics to assess the "quality" of a given simulation in a manner that minimizes potential errors. The objective is to provide a clear set of quantitative implementation requirements for different classes of subgrid models. Efforts have been coordinated as part of recent TNF workshops [23].

The need for improved quality metrics for LES has been recognized now for many years. Activities associated with the TNF Workshop, as one example, has identified many issues. In TNF8 (Heidelberg Germany, 2006), attempts to model simple bluff-body flames (e.g., the "HM1" case) by several different research groups illustrated many ambiguities. Two issues arose from initial comparisons with available experimental data: 1) uncertainty with respect to boundary conditions, and 2) uncertainty with respect to code and simulation parameters (i.e., numerics, grid resolution, time-step, integration time, etc.). Codes with a variety of different numerical schemes and capabilities (e.g., with and without artificial dissipation added for stability) were used. Geometric details of the burner were not resolved. Limited computational resources imposed significant constraints on the levels of spatial and temporal resolution applied. The combined uncertainties made it impossible to draw any conclusions regarding model accuracy. The reason for these ambiguities is due to the fact that all Computational Fluid Dynamics (CFD) calculations are composed of different mathematical elements: 1) numerical methods, 2) physical models, 3) a discretized physical domain, and 4) boundary conditions. Each of these elements introduces uncertainties, and competing

errors interact in a highly nonlinear manner due to the coupled nature of the mathematical systems (see Geurts *et al*. [66]). The broadband multi-scale nature of LES makes it particularly sensitive to these errors. In addition, the integral-scale Reynolds number for most of the validation datasets used (e.g., TNF flames) are of $\mathcal{O}(10^4)$ whereas those associated with most propulsion and power devices are of $\mathcal{O}(10^5)$ or greater. Thus, there is a related need to quantify the effects of increasing Reynolds number and other key quantities on turbulent flame dynamics and understand how to scale validated LES to conditions exhibited at the application level. Accomplishing this hinges on understanding the ranges of scales that a given system of subgrid models accurately operates over and insuring these ranges are not exceeded.

Initial studies aimed at understanding and improving the accuracy of LES focused on the impact of grid resolution on numerical errors and/or model errors. Criteria have been developed to assess LES quality in simple geometries, under simple conditions (single phase, low turbulence intensity, non-reacting). Similarly, various algebraic error indicators (such as Popes 80 % criterion[67]) have been developed in an attempt to provide some guiding metrics (see for example Gant [68] and Celik *et al*. [69]). In TNF9 (Montreal Canada, 2009), algebraic error indicators were applied to the Sydney bluff-body flame (HM1) to explore their utility in the context of the observations above. It was shown that these indicators produce anomalous results. In dissipative schemes, for example, measures of the resolved turbulent kinetic energy in an LES can be misleadingly high since dissipative errors incorrectly damp velocity fluctuations and thus the total level of turbulent kinetic energy in the system. As a consequence, low values of turbulent viscosity suggest good resolution, when in reality artificial dissipation produced non-physical damping of turbulence.

A second focal point in TNF9, followed by TNF10 (Beijing China, 2010), was application of more advanced techniques based on multi-objective optimizations to reach an ideal set of simulation parameters (see for example the pioneering work of Meyers *et al*.[70, 71]). One such technique known as the error-landscape method was applied to the Sydney bluff-body flame (HM1) by Kempf, Geurts, and Oefelein [72]. Results demonstrated how to optimize the Smagorinsky model on a given grid. Small values of the Smagorinsky constant C_s were shown to allow structures to develop in the LES on order of grid spacing where numerical errors dominate. Large values suppressed structures. The optimal value is found in between at C_s = 0.173. The error-landscape method is used to systematically assess the total simulation error that results from the combination of specific models and numerical methods. The novel feature of this method is that it makes use of available experimental data to quantify the error in corresponding simulations. This is in contrast to more sophisticated uncertainty quantification methods that require significantly more input than is typically available from an experiment. The primary advantage of the technique is that it identifies combinations of grid, filter, and model parameters that introduce incorrect flow physics. This allows one to simultaneously minimize the competing effects of these errors. The disadvantage is that combined errors are lumped together and the total error cannot be reduced to arbitrary levels.

A major deficiency with the quality indicators used to date is that none of them account for the various sources of error rigorously. Only the bulk error from multiple competing sources has been considered instead of the distinct sources of error. Discretization and modeling associated with LES introduces three distinct forms of error: 1) discretization errors associated with the numerical techniques; i.e., temporal integration, spatial differencing, and related stabilization schemes, which can induce damping and dispersion of broadband flow processes; 2) the total model residual error,

which is caused by discretization of the sub-models themselves; and 3) the error associated with the model approximation itself due to both the basic assumptions and the related range of subgrid-scales it is specified to work over. Future work will focus on understanding and minimizing these three distinct sources of error and the interactions between them. Quality metrics that relate local grid resolution, the spatial filter size, and corresponding integration time-step to key physical scales such as the Kolmogorov time and length scales, scalar thickness, flame thickness, reaction zone thickness (depending on the flow system of interest) need to be developed that can be used to quantify each of the sources of error individually. Once the errors are quantified, implementation requirements aimed at simultaneously minimizing respective errors and the compounding interactions between them can be developed. To accomplish this goal, a framework similar to that developed by Vervisch *et al*. [73] is required. In contrast to Vervisch *et al*., who focused on developing mesh quality criterion aimed exclusively at minimizing the total model residual error for accurate treatment and analysis of DNS data, the ideas need to be extended with emphasis on treating all three forms of error in the context of LES.

4 Summary

This paper highlights progress toward the application of Large Eddy Simulation (LES) to turbulent multiphase combustion processes typically present in advanced propulsion and power systems. The objective was to provide a systematic analysis of current findings in representative areas and assist in the development of technical performance metrics for model development and validation. Results presented focused on two key areas. The first is the coupling between experiments and LES. The second is on establishing direct links between the idealized jet flame processes (for which significant validation data exists) and extension to application relevant processes exhibited at the device scale. The case studies presented demonstrate current findings in the treatment of the complex thermophysical processes present in advanced systems followed by discussion to add perspective on future needs.

Future work will emphasize three interrelated areas of research: 1) close coordination between LES and the experimental reacting flow research with emphasis on the collaborative activities of the TNF Workshop, 2) initiation of a significant effort in the development of quality assessment techniques for LES aimed at understanding and controlling the myriad of errors that complicate the development and validation of predictive models, and 3) continued development of advanced models and simulation techniques aimed at accurate prediction of multiphase phenomena and turbulent flame behavior across a broad range of combustion modes, regimes, and fuels. Calculations will be performed in a manner that leverages our combined expertise in LES, high performance computing, and access to unique massively parallel computational facilities. Emphasis will be placed on establishing high-fidelity computational benchmarks that identically match the geometry and operating conditions of the selected experimental target flames.

Acknowledgments

Support for this research was provided jointly by the U.S. Department of Energy, Office of Science, Basic Energy Sciences, Division of Chemical Sciences, Geosciences, and Biosciences and the Office of Energy Efficiency and Renewable Energy, Vehicle Technologies Program. The research was performed at the Combustion Research Facility, Sandia National Laboratories, Livermore, California. Sandia National Laboratories is a multiprogram laboratory operated by the Sandia Corporation, a Lockheed Martin Company, for the United States Department of Energy and National Nuclear Security Administration under contract DE-AC- 94AL85000.

References

[1] J. C. Oefelein. *Progress in Aerospace Sciences*, 42 (2006) 2–37.

[2] J. C. Oefelein. *Proceedings of the Combustion Institute*, 30 (2005) 2929–2937.

[3] J. C. Oefelein, R. W. Schefer, and R. W. Barlow. *AIAA Journal*, 44 (2006) 418–433.

[4] J. C. Oefelein. *Combustion Science and Technology*, 178 (2006) 229–252.

[5] J. C. Oefelein, V. Sankaran, and T. G. Drozda. *Proceedings of the Combustion Institute*, 31 (2007) 2291–2299.

[6] T. C. Williams, R. W. Schefer, J. C. Oefelein, and C. R. Shaddix. *Review of Scientific Instruments*, 78 (2007) 035114–1–9. doi: 10.1063/1.27.12936.

[7] R. N. Dahms, L. M. Pickett, and J. C. Oefelein. *Proceedings of the 23rd Annual Conference on Liquid Atomization and Spray Systems*, (2011) journal. Ventura, California.

[8] J. C. Oefelein and G. Lacaze. *Proceedings of the 23rd International Colloquium on the Dynamics of Explosions and Reactive Systems*, (2011) journal. Irvine, California.

[9] B. Hu, M. P. Musculus, and J. C. Oefelein. *Physics of Fluids*, 24 (2012) 1–17. doi: 10.1063/1.3702901.

[10] G. Lacaze and J. C. Oefelein. *Combustion and Flame*, 159 (2012) 2087–2103. doi: 10.1016/j.combustflame.2012.02.003.

[11] J. C. Oefelein, R. N. Dahms, and G. Lacaze. *SAE International Journal of Engines*, 5 (2012) 1–10. doi: 10.4271/2012-10-1258.

[12] J. C. Oefelein, R. N. Dahms, G. Lacaze, J. L. Manin, and L. M. Pickett. *Proceedings of the 12th International Conference on Liquid Atomization and Spray Systems*, (2012) journal. Heidelberg, Germany. ISBN 978-88-903712-1-9.

[13] U. Piomelli. *Progress in Aerospace Sciences*, 35 (1999) 335–362.

[14] R. W. Bilger. *Progress in Energy and Combustion Science*, 26 (2000) 367–380.

[15] D. Veynante and L. Vervisch. *Progress in Energy and Combustion Science*, 28 (2002) 193–266.

[16] J. Janicka and A. Sadiki. *Proceedings of the Combustion Institute*, 30 (2005) 537–547.

[17] H. Pitsch. *Annual Review of Fluid Mechanics*, 38 (2006) 453–482.

[18] V. Bergmann, W. Meier, D. Wolff, and W. Stricker. *Applied Physics B*, 66 (1998) 489–502.

[19] W. Meier, R. S. Barlow, Y.-L. Chen, and J.-Y. Chen. *Combustion and Flame*, 123 (2000) 326–343.

[20] C. Schneider, A. Dreizler, J. Janica, and E. P. Hassel. *Combustion and Flame*, 135 (2003) 185–190.

[21] G.-H. Wang, N. T. Clemens, and P. L. Varghese. *Proceedings of the Combustion Institute*, 30 (2005) 691–699.

[22] G.-H. Wang, N. T. Clemens, and P. L. Varghese. *Applied Optics*, 44 (2005) 6741–6751.

[23] R. S. Barlow. International workshop on measurement and computation of turbulent (non)premixed flames. www.sandia.gov/TNF, 1996-2013. Sandia National Laboratories, Combustion Research Facility, Livermore, California.

[24] G.-H. Wang, R. S. Barlow, and N. T. Clemens. *Proceedings of the Combustion Institute*, 31 (2007) 1525–1532.

[25] G.-H. Wang, A. N. Karpetis, and R. S. Barlow. *Combustion and Flame*, 148 (2007) 62–75.

[26] S. A. Kaiser and J. H. Frank. *Proceedings of the Combustion Institute*, 31 (2007) 1515–1523.

[27] J. H. Frank and S. A. Kaiser. *Experiments in Fluids*, 44 (2008) 221–233. doi: 10.1007/s00348-007-0396-x.

[28] C. Pantano and S. Sarkar. *Physics of Fluids*, 13 (2001) 3803–3819.

[29] J. P. Mellado, S. Sarkar, and C. Pantano. *Physics of Fluids*, 15 (2003) 3280–3307.

[30] J. H. Frank, S. A. Kaiser, and J. C. Oefelein. *Proceedings of the Combustion Institute*, 33 (2011) 1373–1381.

[31] M. Sommerfeld and H.-H. Qiu. *International Journal of Heat and Fluid Flow*, 12 (1991) 20–28.

[32] M. Sommerfeld, A. Ando, and D. Wennerberg. *Journal of Fluids Engineering*, 114 (1992) 648–656.

[33] M. Sommerfeld and H.-H. Qiu. *International Journal of Multiphase Flow*, 19 (1993) 1093–1127.

[34] J. K. Eaton and J. R. Fessler. *International Journal of Multiphase Flow*, 20 (1994) 169–209.

[35] J. D. Kulick, J. R. Fessler, and J. K. Eaton. *Journal of Fluid Mechanics*, 277 (1994) 109–134.

[36] M. R. Maxey and B. K. Patel. *International Journal of Multiphase Flow*, 27 (2001) 1603–1626.

[37] A. Ferrante and S. E. Elghobashi. *Physics of Fluids*, 15 (2003) 315–329.

[38] M. Oschwald, J. Smith, R. Branam, J. Hussong, A. Schik, B. Chehroudi, and D. Talley. *Combustion Science and Technology*, 178 (2006) 49–100.

[39] M. Habiballah, M. Orain, F. Grisch, L. Vingert, and P. Gicquel. *Combustion Science and Technology*, 178 (2006) 101–128.

[40] K.-C. Lin, S. Cox-Stouffer, and T. Jackson. *Combustion Science and Technology*, 178 (2006) 129–160.

[41] S. Candel, M. Juniper, G. Singla, P. Scouflaire, and C. Rolon. *Combustion Science and Technology*, 178 (2006) 161–192.

[42] N. Zong and V. Yang. *Combustion Science and Technology*, 178 (2006) 193–228.

[43] J. Bellan. *Combustion Science and Technology*, 178 (2006) 253–281.

[44] L. C. Selle, N. A. Okong'o, J. Bellan, and K. G. Harstad. *Journal of Fluid Mechanics*, 593 (2007) 57–91.

[45] G. Ribert, N. Zong, V. Yang, L. Pons, N. Darabiha, and S. Candel. *Combustion and Flame*, 154 (2008) 319–330.

[46] G. Lacaze, B. Cuenot, T. Poinsot, and M. Oschwald. *Combustion and Flame*, 156 (2009) 1166–1180.

[47] L. Pons, N. Darabiha, S. Candel, G. Ribert, and V. Yang. *Combustion Theory and Modelling*, 13 (2009) 57–81.

[48] T. Schmitt, Y. Méry, M. Boileau, and S. Candel. *Proceedings of the Combustion Institute*, 33 (2011) 1383–1390.

[49] T. W. Leland and P. S. Chappelear. *Industrial and Engineering Chemistry Fundamentals*, 60 (1968) 15–43.

[50] J. S. Rowlinson and I. D. Watson. *Chemical Engineering Science*, 24 (1969) 1565–1574.

[51] R. C. Reid, J. M. Prausnitz, and B. E. Polling. *The Properties of Liquids and Gases*. McGraw-Hill, New York, New York, 4th edition, 1987.

[52] G. J. VanWylen and R. E. Sonntag. *Fundamentals of Classical Thermodynamics*. John Wiley and Sons, Incorporated, New York, New York, 3rd edition, 1986.

[53] S. Gordon and B. J. McBride. Computer program for calculation of complex chemical equilibrium compositions, rocket performance, incident and reflected shocks and Chapman-Jouguet detonations. Technical Report NASA SP-273, National Aeronautics and Space Administration, 1971.

[54] R. J. Kee, F. M. Rupley, and J. A. Miller. Chemkin thermodynamic data base. Technical Report SAND87-8215B, Sandia National Laboratories, 1990. Supersedes SAND87-8215 dated April 1987.

[55] J. F. Ely and H. J. M. Hanley. *Industrial and Engineering Chemistry Fundamentals*, 20 (1981) 323–332.

[56] J. F. Ely and H. J. M. Hanley. *Industrial and Engineering Chemistry Fundamentals*, 22 (1981) 90–97.

[57] R. B. Bird, W. E. Stewart, and E. N. Lightfoot. *Transport Phenomena*. John Wiley and Sons, Incorporated, New York, New York, 1960.

[58] J. O. Hirschfelder, C. F. Curtiss, and R. B. Bird. *Molecular Theory of Gases and Liquids*. John Wiley and Sons, Incorporated, New York, New York, 2nd edition, 1964.

[59] S. Takahashi. *Journal of Chemical Engineering of Japan*, 7 (1974) 417–420.

[60] J. W. Cahn and J. E. Hilliard. *Journal of Chemical Physics*, 28 (1958) 258–267.

[61] E. A. Müller and A. Mejía. *Fluid Phase Equilibria*, 282 (2009) 68–81. doi: 10.1016/j.fluid.2009.04.022.

[62] A. Mejía, J. C. Pàmies, D. Duque, H. Segura, and L. F. Vega. *Journal of Chemical Physics*, 123 (2005) 1–10. doi: 10.1063/1.1955529.

[63] C. Miqueu, J. M. Míguez, M. M. Piñeiro, T. Lafitte, and B. Mendiboure. *Journal of Physical Chemistry B*, 115 (2011) 9618–9625. doi: 10.1021/jp202276k.

[64] L. M. Pickett. Engine combustion network. www.sandia.gov/ECN, 2005-2013. Sandia National Laboratories, Combustion Research Facility, Livermore, California.

[65] R. N. Dahms, J. Manin, L. M. Pickett, and J. C. Oefelein. *Proceedings of the Combustion Institute*, 34 (2013) 1667–1675. doi: 10.1016/j.proci.2012.06.169.

[66] B. J. Geurts and J. Fröhlich. *Physics of Fluids*, 14 (2002) 41–44. doi: 10.1063/1.1480830.

[67] S. B. Pope. *Turbulent Flows*. Cambridge University Press, Cambridge, United Kingdom, 2000.

[68] S. E. Gant. *Flow, Turbulence and Combustion*, 84 (2010) 325–335. doi: 10.1007/s10494-009-9237-8.

[69] I. B. Celik, Z. N. Cehreli, and I. Yavuz. *Journal of Fluids Engineering*, 127 (2005) 949–958.

[70] J. Meyers, B. J. Geurts, and M. Baelmans. *Physics of Fluids*, 15 (2003) 2740–2755. doi: 10.1063/1.1597683.

[71] J. Meyers, P. Sagaut, and B. J. Geurts. *Physics of Fluids*, 18 (2006) 1–12. doi: 10.1063/1.2353402.

[72] A. M. Kempf, B. J. Geurts, and J. C. Oefelein. *Combustion and Flame*, 158 (2011) 2408–2419. doi: 10.1016/j.combustflame.2011.04.012.

[73] L. Vervisch, P. Domingo, G. Lodato, and D. Veynante. *Combustion and Flame*, 157 (2010) 778–789. doi: 10.1016/j.combustflame.2009.12.017.